

Influence of microstructures on thermal fatigue property of a nickel-base superalloy

Peng-Cheng XIA (✉)^{1,2}, Feng-Wen CHEN¹, Kun XIE¹, Ling QIAO¹, and Jin-Jiang YU²

¹ College of Materials Science and Engineering, Shandong University of Science and Technology, Qingdao 266590, China

² Institute of Metal Research, Chinese Academy of Sciences, Shenyang 110016, China

© Higher Education Press and Springer-Verlag Berlin Heidelberg 2015

ABSTRACT: Effect of microstructures such as the distribution and shape of carbide and γ' phase on thermal fatigue property of a superalloy was investigated experimentally. The resistance of thermal fatigue of the studied alloy decreases with the rising upper temperature. For the as-cast alloy, the thermal fatigue crack mostly originates from carbide at low upper temperature and results from oxidation at high upper temperature. The thermal fatigue crack of the heat treated alloy is mainly initiated by the oxidized cavity and then propagates through the join of the oxidized cavity. The orientation of crack propagation and direction of dendrite growth of alloy have the angle of 45° . There is γ' denuded region near the thermal fatigue crack because of oxidation.

KEYWORDS: nickel-base superalloy; thermal fatigue; microstructure; crack

Contents

- 1 Introduction
 - 2 Experiment and methods
 - 3 Results and discussion
 - 3.1 Microstructure of the alloy
 - 3.2 The effect of microstructure on thermal fatigue property
 - 4 Conclusions
- Abbreviations
Acknowledgements
References

1 Introduction

Superalloys are widely used in various applications with

aggressive atmospheres, such as jet engine, gas turbine etc. [1–2]. They chronically work at 650°C – 1200°C with sophisticated stress. Thermal fatigue is one of the potential modes of failure in many components of superalloys such as vanes, blades etc., which are exposed to the fluctuating temperature [3]. The property of thermal fatigue resistance should firstly be considered when selecting alloys for a fluctuating temperature application. At present, the evaluation of thermal fatigue resistance property is not yet standardized at home and abroad. The main reason is that a thermal cycle may not result in the same stress because of different specimen shape and heating and cooling rate. Therefore it is difficult to compare thermal fatigue property of an alloy through different investigations. Previous experiment results show that the thermal fatigue property of an alloy is greatly influenced by the following factors, upper temperature, specimen shape, notched radius and direction, holding time and microstructure [4–10]. There are a few literatures about thermal fatigue property of superalloy. The material used in this investigation is a

directionally solidified nickel-base superalloy, which is potentially used as vane material. It is essential to have a thorough understanding of the thermal fatigue property of such an alloy and explore the role of many parameters such as upper temperature and microstructure.

2 Experiment and methods

The chemical compositions of experimental materials in this work is (wt.%): 0.05C, 9.0Cr, 5.0Co, 6.0Al, 3.0W, 3.0Mo, 2.2Nb, and bal. Ni. The master alloy was first melted in a vacuum induction furnace. Directionally solidified specimens with the direction of [001] then were made by the HRS (high rate solidification) method in a ZGD2 type vacuum furnace with a temperature gradient of $(70\text{--}90)^\circ\text{C}\cdot\text{cm}^{-1}$ and a withdrawal rate of $5\text{ mm}\cdot\text{min}^{-1}$. The alloy was heat treated in order to investigate the influence of microstructure on thermal fatigue property. The process of heat treatment was 1220°C , 4 h/AC (air cooling) + 1150°C , 4 h/AC + 870°C , 24 h/AC.

Figure 1 shows the schematic diagram of thermal fatigue specimen with V-type notch. All samples were mechanically polished and carefully examined before test so as to eliminate the residual stress around the notch. Specimen was first heated to the upper temperatures of 1000°C , 1050°C and 1100°C respectively and held for the set time. The total time of heating and holding time was 10 min. Then the specimen was cooled to room temperature (RT) in water and the cooling time was 30 s. The thermal cycling tests were interrupted periodically and specimens were polished. The lengths of the longest crack at both sides of specimen were measured with a reading-scale lens. The given lengths of the longest crack were an average of six cracks or more at a specimen experienced the same thermal cycling test. The cycling numbers of crack initiation was defined the cycles when the crack length was about $200\ \mu\text{m}$. Microstructure was examined by scanning electron microscopy (SEM).

3 Results and discussion

3.1 Microstructure of the alloy

The as-cast alloy (AS alloy) has MC-type carbide and the morphology of carbide is script-like (Fig. 2(a)). After heat treatment, the MC carbide changes into blocky particles and discontinuously distributes in interdendrite region or

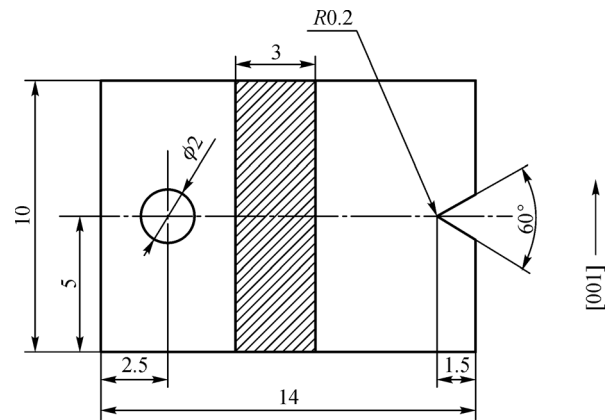


Fig. 1 Schematic diagram of the thermal fatigue specimen of alloy (unit: mm).

grain boundary (Fig. 2(b)). The γ' phase of the AS alloy is irregular cubic and has the size of about 390 nm. The volume fraction of γ' phase is about 60% (Fig. 3(a)). There are different shape and size of γ' precipitates of the heat treated alloy (HT alloy) (Fig. 3(b)). The diameter of spherical γ' phase is approximately 160 nm, while the cuboidal γ' phase has the size of about 760 nm. The volume fraction of bimodal γ' precipitates is about 68%.

There are bimodal γ' precipitates after heat treatment (Fig. 3(b)), which demonstrates that the aging temperature of high temperature (1150°C) is between the initial solution temperature and fully solution temperature of γ' precipitates. Partial γ' phase again solutes into matrix, then small and spherical γ' particles precipitate during the following cooling. On the other hand, it is advantageous for γ' phase to grow because of quick diffusion rate of elements at elevated aging temperature. The γ' precipitates which do not solute into matrix begin to grow up and shift to cubical.

3.2 The effect of microstructure on thermal fatigue property

Initiation numbers of thermal fatigue crack at different upper temperatures are listed in Table 1. The alloy has higher cycles of crack initiation at low upper temperature. The thermal fatigue resistance property decreases and crack initiation numbers dramatically reduce with the increasing upper temperature. This shows that the fatigue property of the alloy is better at low upper temperature. Table 1 indicates that the small thermal fatigue cracks are generated after tens of thermal cycles. It demonstrates that the crack initiation requires an incubation period [9–10]. The crack initiation time is related to the microstructure and property of alloy.

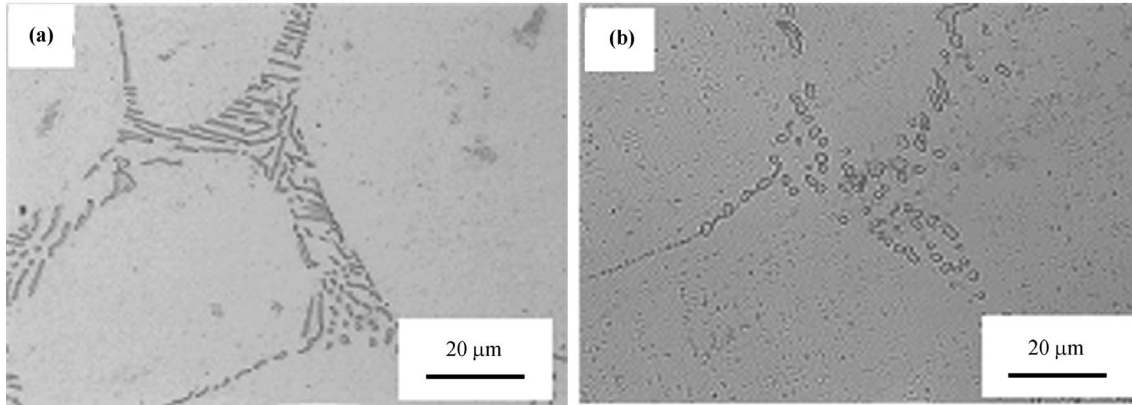


Fig. 2 The carbide morphology of (a) AS alloy and (b) HT alloy.

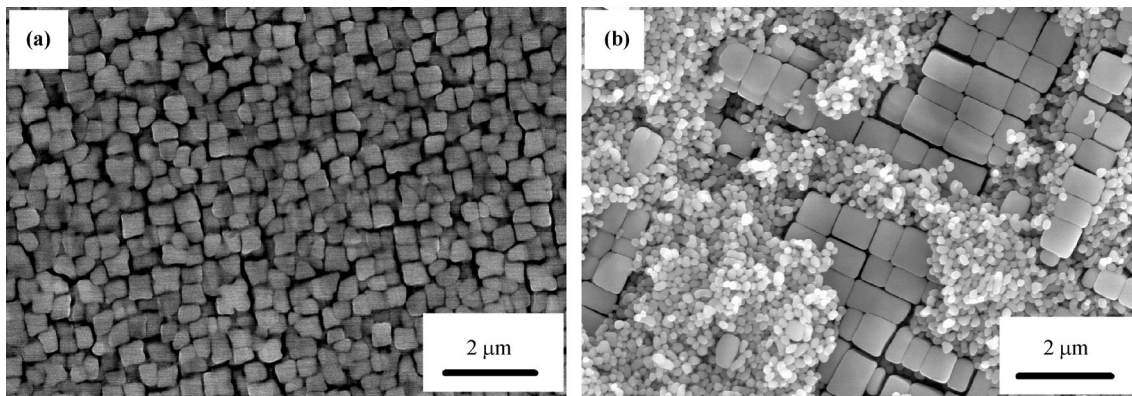


Fig. 3 The γ' precipitate of (a) AS alloy and (b) HT alloy.

Table 1 Initiation cycles of thermal fatigue crack at different upper temperatures

Cycle temperature	Initiation cycles	
	AS alloy	HT alloy
1000°C↔RT	46	58
1050°C↔RT	40	53
1100°C↔RT	24	33

It may be valuable to note that the crack initiation numbers drops slightly when the temperature rises from 1000°C to 1050°C. The crack initiation numbers drops sharply when the temperature increases up to 1100°C, meaning that thermal fatigue property of alloy is sensitive to high temperature.

The temperature distribution is uneven at the whole specimen during heating. The temperature of the specimen surface firstly increases. The temperature of the specimen centre is low. The specimen surface expands. The centre restricts the expansion of the surface, which generates tensile stress. On the contrary, compressive stress is generated during cooling. The thermal stress which is induced by thermal cycles has great influence on the

initiation numbers of fatigue crack. The thermal stress σ can be expressed as follows:

$$\sigma = \alpha E \Delta T \quad (1)$$

where α is the linear expansion coefficient, E is the modulus of elasticity, and ΔT is the temperature range of the surface temperature and centre temperature. Many experimental results [5,11] demonstrate that ΔT increases with the rising temperature (heating) or dropping temperature (cooling). Then ΔT shortens when the temperature distribution in the whole specimen becomes even. The higher the upper temperature, the greater the ΔT . It is easy to conclude from Eq. (1) that with the increase of upper temperature, the thermal stress becomes greater as well. This, at least in partially, can explain the reduced crack initiation life with the lift of upper temperature. It is also well known that the strength of most nickel-base superalloys falls dramatically in the testing temperature range. These effects will attribute to the decrease of thermal fatigue resistance with increasing upper temperature. Moreover, it is certain that with the increase of upper temperature, high temperature oxidation behavior will play

a more significant role in affecting the crack initiation behavior.

There are some small cracks around notch during crack initiation period for AS alloy at low upper temperature (Fig. 4(a)). Fatigue cracks of AS alloy initiate by carbides (Fig. 4(b)). As shown in Fig. 4(b), there are many small holes around the carbides. Thermal fatigue cracks initiate by the join of small holes. The crack propagates along the carbide during the thermal cycling test. It is known that

there are the script-like carbides in AS alloy and more importantly the carbides continuously distribute in interdendrite region or grain boundary (Fig. 2(a)). The difference in the expanding coefficient between the matrix and the carbide easily results in large inter-stress at the interface during thermal fatigue test. The higher the temperature, the larger the inter-stress. It will cause a few small cracks at the interface when the inter-stress exceeds the binding strength between matrix and the carbide at high

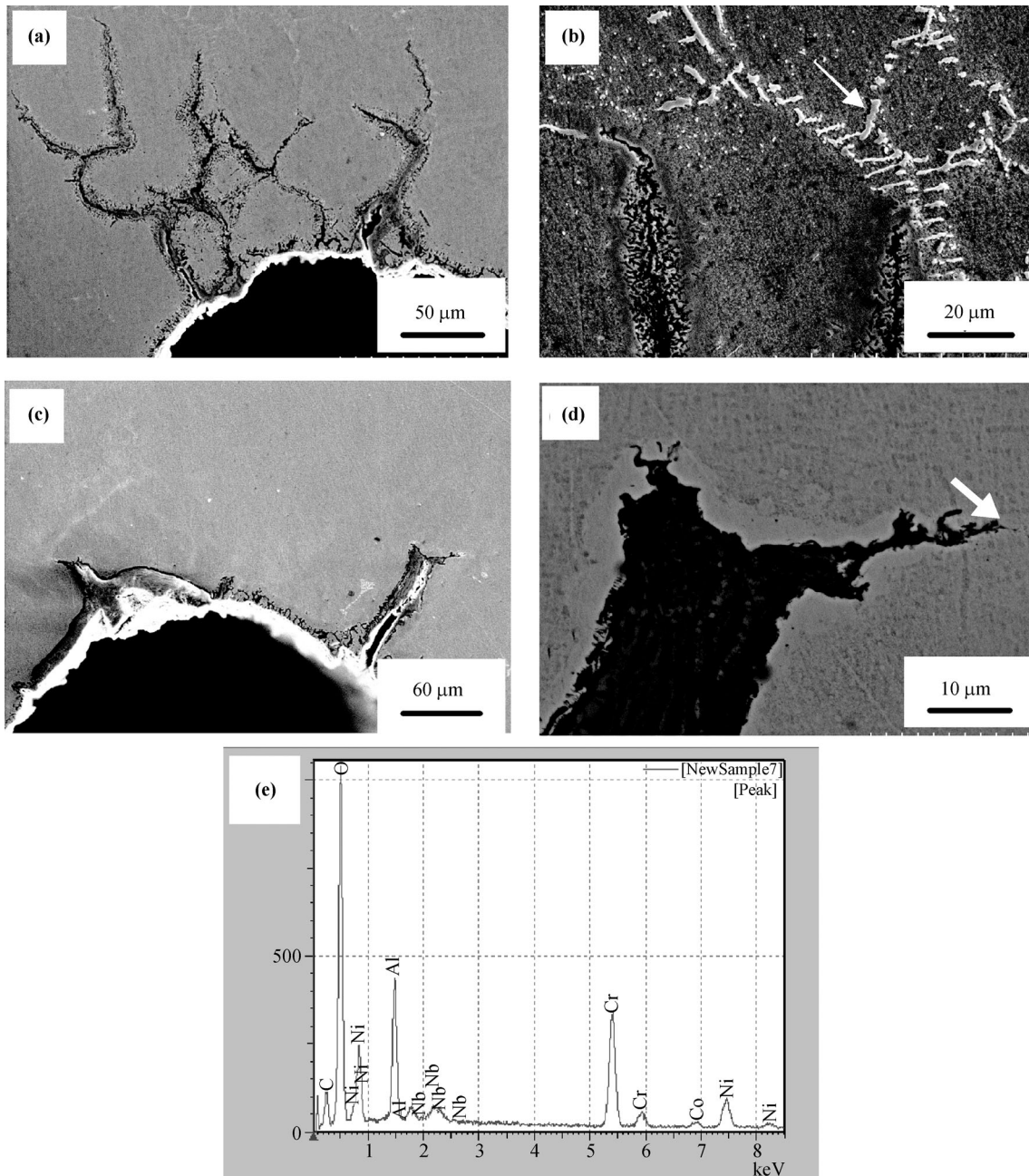


Fig. 4 Crack initiation of alloy at upper temperature of 1000°C: (a) thermal fatigue cracks of AS alloy; (b) crack initiation of AS alloy by carbide; (c) thermal fatigue cracks of HT alloy; (d) crack initiation of HT alloy by oxidation. (e) EDS result corresponding to the region of crack tip indicated by the arrow in (d).

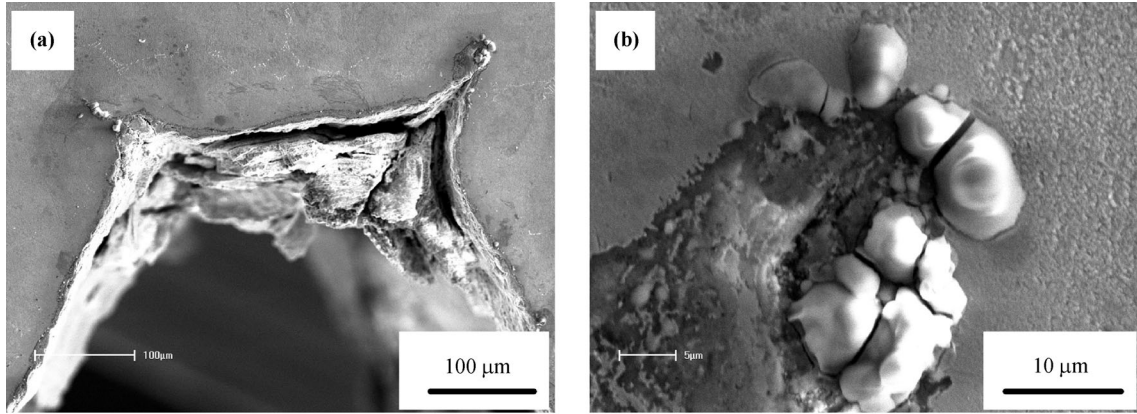


Fig. 5 Crack initiation of AS alloy at upper temperature of 1100°C: (a) thermal fatigue cracks; (b) oxide and holes near crack.

temperature (indicated by the arrow in Fig. 4(b)). On the other hand, the MC-type carbides of script-like are easy to be oxidized and separate from matrix, so that they become cracks nucleation sites. The larger crack creates by combining small cracks. It is easy for the thermal crack to propagate along the direction of carbide distribution. Therefore, AS alloy has short initiation life of thermal fatigue.

HT alloy has two large cracks in the initiation stage at the upper temperature of 1000°C (Fig. 4(c)). The crack is wide and deep. There are no fatigue cracks around carbides. Crack of thermal fatigue initiates by oxidization. There are many small holes near the crack tip (Fig. 4(d)). Energy dispersive spectroscopy (EDS) result (Fig. 4(e)) in the region of crack tip (indicated by the arrow in Fig. 4(d)) shows that they are rich in Al, Cr, O and Ni elements. Al and Cr elements are easy to oxidize and form oxide. The oxides attach themselves to the surface of alloy. There is inter-stress in the surface between alloy and oxide with the rising temperature for the difference of in expanding coefficient. The larger the inter-stress, the higher the temperature. The oxide desquamates from the alloy when the inter-stress exceeds the binding force between oxide and alloy. The volume fraction of γ' phase near oxide decreases for the reduction of Al content, which results in the low strength near oxide. It is easy to form small oxide holes. The fatigue crack initiate by the join of holes.

The fatigue cracks of AS alloy and HT alloy initiate at high upper temperature by oxidation. Figure 5 demonstrates crack initiation of the AS alloy at upper temperature of 1100°C. Figure 5(a) shows that there are no cracks around carbides. There are many oxides in the crack tip and holes near crack (Fig. 5(b)).

Thermal fatigue crack propagates with the increase of

cycles after crack initiation. Kinetics curves of crack propagation of thermal fatigue with different upper temperatures are shown in Fig. 6. It indicates that the resistance of thermal fatigue reduces with the rise of upper temperature. The length of thermal fatigue crack of alloy after 150 cycles is listed in Table 2, which shows that the length of fatigue crack rises with the increase of upper temperature.

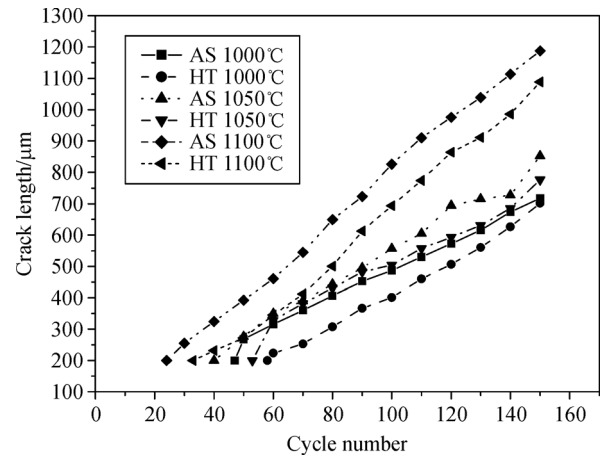


Fig. 6 Kinetics curves of crack propagation of thermal fatigue at different upper temperatures.

Table 2 Crack length of thermal fatigue after 150 cycles at different upper temperatures

Cycle temperature	Crack length / μm	
	AS alloy	HT alloy
1000°C \leftrightarrow RT	679	1786
1050°C \leftrightarrow RT	812	1823
1100°C \leftrightarrow RT	1187	2215

Mechanical mechanism is applied to explain the phenomenon. If the initial crack is considered as a short

crack, a local stress intensity factor ΔK created by stress field of a V-type notch might be applied and an initial crack might firstly be generated at the site where the local maximal stress intensity factor, ΔK_{\max} , is higher than the threshold value of fatigue crack propagation, ΔK_{th} [12]. The ΔK is proportion to $\Delta\sigma$ ($\Delta\sigma$ is the stress difference) according to the ΔK computational formula. From Eq. (1), it is not difficult to conclude that the stress difference $\Delta\sigma$ becomes higher with the rise of upper temperature. Therefore, the larger the ΔK , the higher the upper temperature. It is easy for fatigue cracks to propagate at high upper temperature so that the length of fatigue crack rises with the increase of upper temperature. Calculation of ΔK_{\max} under local condition is possible by thermal and stress field measurements and calculations. The quantitative study on thermal fatigue cracks has not been published till now. Reger et al. provided a new method to test the stress and strain of alloy during thermal cycles by pulsed eddy current (PEC) and magnetic Barkhausen emission (MBE) [12]. The thermal fatigue property of alloy can be quantitatively measured soon.

Thermal fatigue cracks of AS alloy and HT alloy after

150 cycle numbers at different upper temperatures are shown in Fig. 7. AS alloy and HT alloy have two cracks of thermal fatigue.

The thermal fatigue crack of AS alloy is wide (Figs. 7(a) and 7(c)). There are not cracks around carbides, indicating that the crack propagation is not through carbides. The join of oxidation holes makes crack grow. Figure 6(d) shows the crack propagation of HT alloy with the upper temperature of 1100°C. There are many holes around fatigue crack. Some holes join each other, which forms crack. The crack propagation is by join of oxide holes.

It is interesting to note that the orientation of crack propagation and direction of dendrite growth of the alloy have some angle. The angle between the orientation of crack propagation and direction of dendrite growth is 45° by measurement. The {111} face is the close-packed face of face-centered cubic crystal in the course of propagation of fatigue crack. The direction of $\langle 110 \rangle$ is the close-packed direction of {111} face. It is the common slip system of face-centered cubic crystal. Two propagation directions $\langle 110 \rangle$ of thermal fatigue crack are the direction of the maximum shear stress if the notch is regarded as the pre-

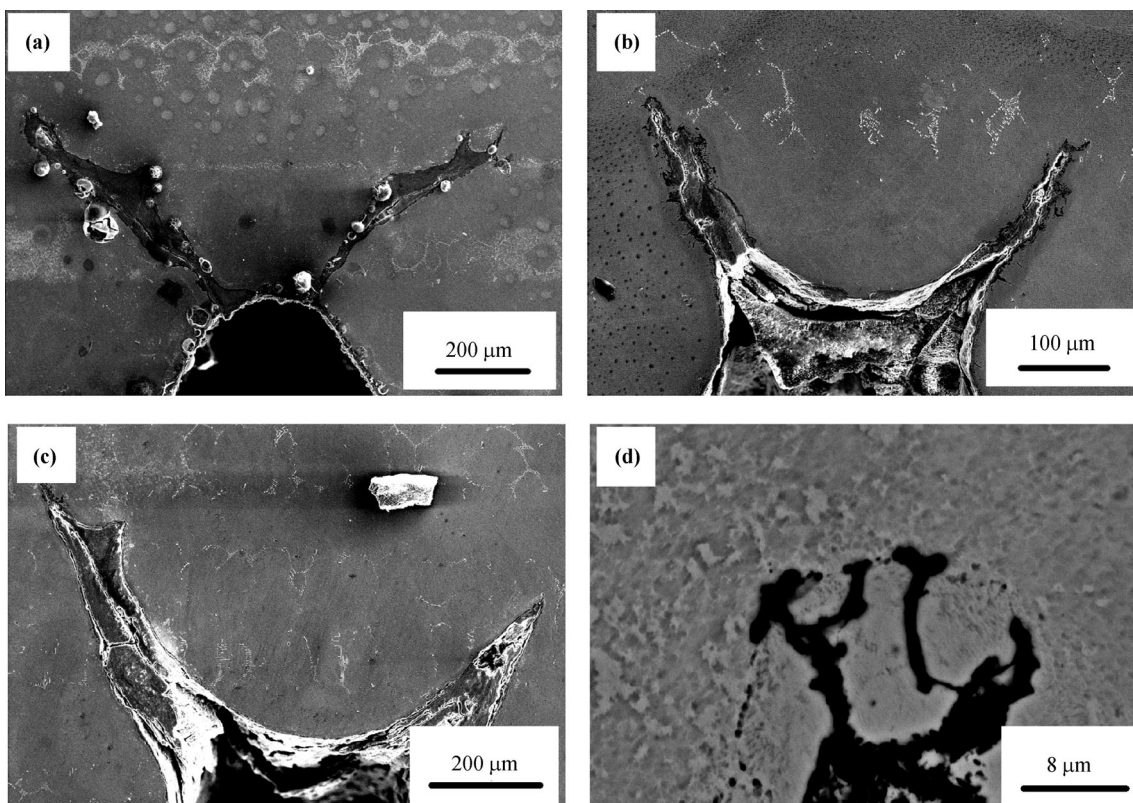


Fig. 7 Crack propagation of thermal fatigue with different upper temperatures after 150 cycles: (a) thermal fatigue crack of AS alloy at 1000°C; (b) thermal fatigue crack of HT alloy at 1050°C; (c) thermal fatigue crack of AS alloy at 1100°C; (d) oxidized cavity of AS alloy at 1100°C.

crack in this experiment. It is easy for thermal fatigue crack to propagate along two directions $\langle 110 \rangle$ because of large stress.

There is γ' denuded region near cracks after thermal fatigue experiment (indicated by arrows in Figs. 8(a) and 8(b)). The result of the line scanning indicates that the content of Al and Cr drops and the content of Ni increases in some regions (BC and DE in Fig. 8(c)), which shows that γ' denuded phenomenon is related to oxidation. The elements near fatigue cracks are unstable. It is easy for Cr and Al elements to combine with O in air and form oxide during thermal fatigue test. There is large inter-stress in the interface of alloy and the oxide because of the difference of dilatation coefficient at high temperature. Oxide desquamates from the alloy surface for large thermal stress at higher temperature. Cr and Al elements continue to oxidize so that the contents of Cr and Al gradually reduce near thermal fatigue cracks and the γ' volume fraction decreases with the drop of Al element. The more

sufficient the oxidization course, the longer the exposure time at high temperature. The solid solubility of γ' precipitate in the matrix increases for the lessening of Cr element near crack, which further drops γ' volume fraction. There is γ' denuded region near thermal fatigue cracks. It is inevitable for the microstructure evolution to occur during the thermal fatigue test. The γ' phase coarsens and rafts (Fig. 8(a)). The γ' rafting is related to the alternating temperature and thermal stress in the course of thermal fatigue [13].

The HT alloy has superior thermal fatigue property than that of the AS alloy. The volume fraction of γ' phase raises and dendritic segregation decreases after heat treatment, which improves the HT alloy strength. The critical stress that thermal fatigue crack propagates along $[110]$ direction increases. The larger stress is required when crack spreads, which enhances the fatigue property of HT alloy. The carbide of HT alloy changes blocky particles and discontinuously distributes in interdendrite region or

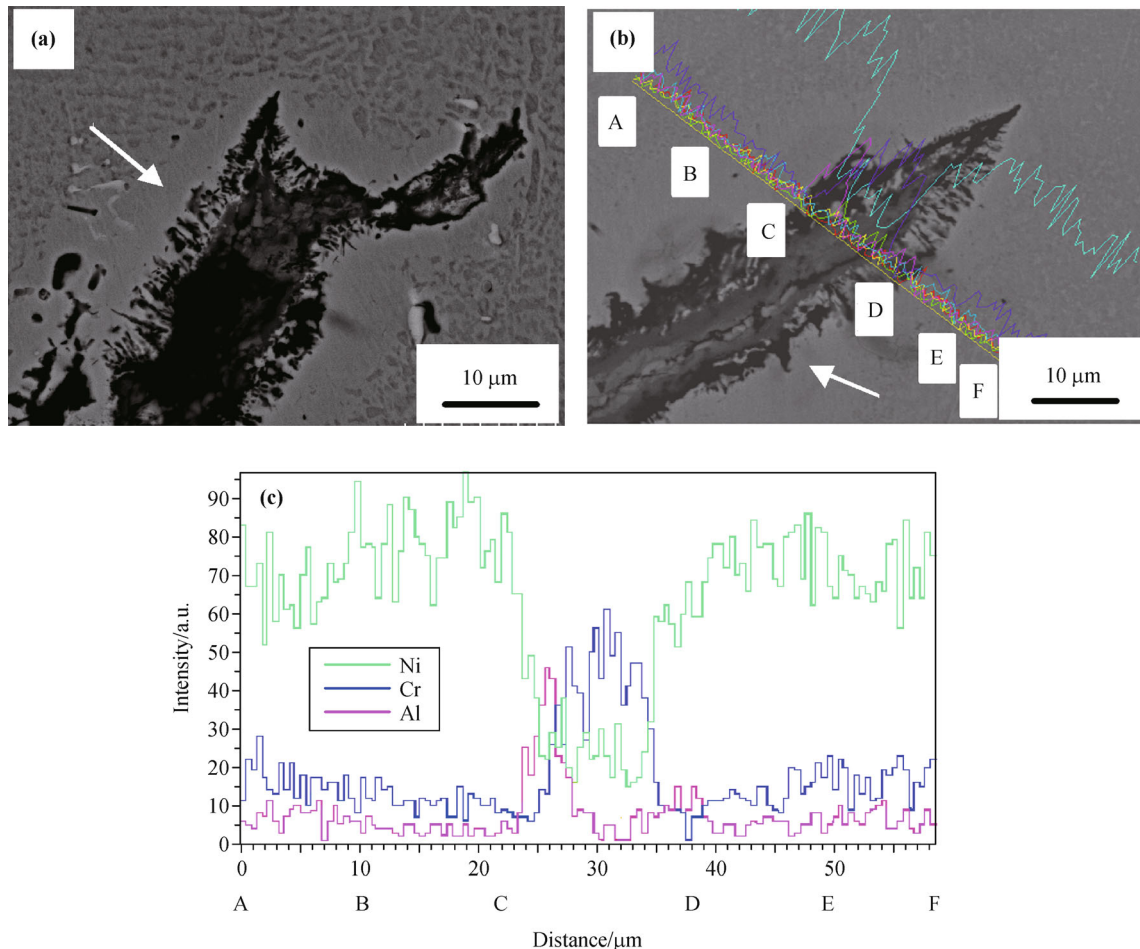


Fig. 8 The γ' denuded region during thermal fatigue test: (a) HT alloy at the upper temperature of 1050°C; (b) AS alloy at the upper temperature of 1000°C. (c) Line scanning corresponding to the γ' denuded region in AS alloy.

grain boundary, which inhibits the initiation and propagation of fatigue crack.

4 Conclusions

1) As-cast alloy has script-like carbide and irregular cubic γ' precipitates. The carbide changes to block and discontinuously distributes in interdendrite region or grain boundary by heat treatment. There are bimodal γ' precipitates of heat treated alloy.

2) Cycles of crack initiation shorten and resistance of thermal fatigue reduces with the raise of upper temperature. As-cast alloy initiates thermal fatigue crack by carbide at low upper temperature and by oxidation at high upper temperature. Crack initiation of heat treated alloy is mainly by oxidized cavity. The join of oxidized holes makes crack propagate. Heat treated alloy has excellent thermal fatigue property.

3) The orientation of crack propagation and direction of dendrite growth of alloy have the angle of 45° . There is γ' denuded region near thermal fatigue crack because of oxidation during thermal fatigue test.

Abbreviations

AC	air cooling
AS alloy	as-cast alloy
EDS	energy dispersive spectroscopy
HRS	high rate solidification
HT alloy	heat treated alloy
MBE	magnetic Barkhausen emission
PEC	pulsed eddy current
RT	room temperature
SEM	scanning electron microscopy

Acknowledgements This work was financially supported by Research Award Fund for Outstanding Young and Middle-aged Scientists of Shandong Province in China (BS2011CL032), Taishan Scholars Project of Shandong (ts20110828), the State Key Laboratory of Mining Disaster Prevention and Control Co-founded by Shandong Province and the Ministry of Science and Technology, Shandong University of Science and Technology (MDPC2013KF15), and the National Natural Science Foundation of China (Grant Nos. 51272141 and 51208288). The authors are grateful for those supports.

References

- [1] Sims C T, Stoloff N S, Hagrel W C. Superalloys II. New York, USA: John Wiley & Sons, 1987
- [2] Matthew J, Donachie J. Superalloy. Ohio, USA: American Society for Metals, 1984
- [3] Mansoor M, Ejaz N. Thermal fatigue failure of fuel spray bars of a jet engine afterburner. *Engineering Failure Analysis*, 2011, 18(1): 492–498
- [4] Woodford D A, Mowbray D F. Effect of material characteristics and test variables on thermal fatigue of cast superalloy. *Materials Science and Engineering*, 1974, 16(1–2): 5–43
- [5] Glenny E, Taylor T A. A study of the thermal-fatigue behavior of metals: The effect of test conditions on nickel-base high-temperature alloys. *Journal of the Institute of Metals*, 1959–1960, 88: 449–461
- [6] Felberbaum L, Voisey K, Gaumann M, et al. Thermal fatigue of single-crystalline superalloy CMSX-4R: A comparison of epitaxial laser-deposited material with the base single crystal. *Materials Science and Engineering A*, 2001, 299(1–2): 152–156
- [7] Bhattachar V S. Thermal fatigue behaviour of nickel-base superalloy 263 sheets. *International Journal of Fatigue*, 1995, 17(6): 407–413
- [8] Francois M, Remy L. Influence of microstructure on the thermal fatigue behavior of a cast cobalt-base superalloy. *Metallurgical Transactions A*, 1990, 21(3): 949–958
- [9] Liu Y, Yu J J, Xu Y, et al. Crack growth behavior of SRR99 single crystal superalloy under thermal fatigue. *Rare Metals*, 2008, 27(5): 526–530
- [10] Yang J X, Zheng Q, Sun X F, et al. Thermal fatigue behavior of K465 superalloy. *Rare Metals*, 2006, 25(3): 202–209
- [11] Mowbray D F, Mcconnelee T E. Nonlinear analysis of a tapered disk thermal fatigue specimen. In: Spera D A, Mowbray D F, eds. *Thermal Fatigue of Materials and Components*. West Conshohocken, PA: America Society for Testing and Materials, 1976, 10–29
- [12] Reger M, Remy L. High temperature, low cycle fatigue of IN-100 superalloy: Influence of temperature on the low cycle fatigue behaviour. *Materials Science and Engineering A*, 1988, 101: 47–54
- [13] Xia P C, Yang L, Yu J J, et al. Microstructural evolution of a directionally solidified nickel-base superalloy during thermal fatigue. *Rare Metals*, 2011, 30(S): 477–481